

Non-monotonic dynamic correlations beneath the surface of glass-forming liquids

Hailong Peng,^{1,*} Huashan Liu,¹ and Thomas Voigtmann^{2,3,†}

¹*School of Materials Science and Engineering, Central South University, 932 South Lushan Rd, 410083 Changsha, China*

²*Institut für Materialphysik im Weltraum, Deutsches Zentrum für Luft- und Raumfahrt (DLR), 51170 Köln, Germany*

³*Department of Physics, Heinrich-Heine-Universität Düsseldorf,*

Universitätsstraße 1, 40225 Düsseldorf, Germany

(Dated: July 13, 2021)

Collective motion over increasing length scales is a signature of the vitrification process of liquids. We demonstrate how distinct static and dynamic length scales govern the dynamics of vitrifying films. In contrast to a monotonically growing static correlation length, the dynamic correlation length that measures the extent of surface-dynamics acceleration into the bulk, displays a striking non-monotonic temperature evolution that is robust also against changes in detailed interatomic interaction. This non-monotonic change defines a cross-over temperature T_* that is distinct from the critical temperature T_c of mode-coupling theory (MCT). We connect this non-monotonic change to a cross-over from mean-field like liquid dynamics to glass-like dynamics that is signalled by a morphological change of cooperative rearrangement regions (CRR) of fast particles, and as the point where fast-particle motion decouples from structural relaxation. We propose a rigorous definition of this new cross-over temperature T_* within a recent extension of MCT, the stochastic β -relaxation theory (SBR).

Dynamical processes in a liquid close to the glass transition become cooperative across spatial regions of increasing extent [1], and it is thus natural to seek an intrinsic correlation length whose divergence would signal the transition. But the hallmark of the glass transition is a dramatic change in the dynamics that is caused by only weak changes in the statics. Consistently, attempts at defining *static* correlation lengths have found only weak changes in these quantities close to the (computationally or experimentally accessible part) of the transition [1–4]. Only recently it has become clear that in certain perturbed systems, *dynamic* correlation lengths can be defined that display a much more interesting, non-monotonic behavior [5–7] with a peak at some cross-over temperature. Such non-monotonic variations near the glass transition have since emerged as a signature of various non-equilibrium glass-forming systems [8, 9].

The prevailing methodology to detect spatial correlations in glassy systems is suggested by the random first-order theory (RFOT) [10–12]: pinning a subset of particles in the equilibrium fluid, one examines how the configuration of the rest of particles is influenced [13–16]. While this point-to-set (PTS) protocol is designed to keep the *static* properties of the system in equilibrium, it represents a strong perturbation of the dynamics [17]: The freezing of some particles can be viewed as imposing a zero-temperature region and hence a strong temperature gradient, yet the associated linear-response regime shrinks to zero at the glass transition [18]. We propose the study of glassy films as a new method to detect such dynamic correlation lengths by measuring how far the statics and dynamics into the bulk liquid affected by the accelerated mobility on the surface.

We show here that the dynamics in *equilibrated films* is similarly governed by a non-monotonically dynamical correlation length. This opens an interesting link between the study of such films and our fundamental understanding of the glass transition in the bulk, in analogy to the situation that the diverging width of a gas–liquid interface at its critical point is governed by the same diverging correlation length in the bulk [19]. Furthermore the free-surface dynamics is an important factor in the preparation of glassy films [20–22], and more specifically ultra-stable glasses [23–27] and nanostructured materials [28] that are produced by depositing atoms layer-by-layer on an amorphous substrate.

We demonstrate that a specific cross-over temperature T_* governs both the point of maximal dynamical correlations in the film geometry, and the point where cooperative rearrangement regions (CRR) of fast particles in the bulk undergo a shape transition. This cross-over point T_* is significantly above the critical temperature T_c of the mode-coupling theory (MCT). We rationalize this new cross-over point in the context of a recent extension of MCT, the stochastic β -relaxation theory (SBR), as the point where the effect of long-range fluctuations in the dynamical order parameter of the theory is most pronounced in decoupling fast-particle dynamics from bulk relaxation.

We study two exemplary glass formers by molecular dynamics (MD) simulations: the Kob-Andersen Lennard-Jones binary mixture (LJBM) [29] showing weak surface layering, and a model of the molten CuZr alloy with embedded-atom method (EAM) many-body interactions [30] showing strong layering. Simulations (using the LAMMPS package [31]) start in the bulk liquid at high temperature ($T = 0.6$ for LJBM; $T = 2000$ K for CuZr) and zero pressure. A liquid-vacuum interface was created by an instantaneous increase of the box length along the z -axis [see the illustration in Fig. 1(a)]. Af-

* hailong.peng@csu.edu.cn

† thomas.voigtmann@dlr.de

ter re-equilibration, the membranes were cooled down to subsequently lower target temperatures in the canonical ensemble (NVT); data was collected in the microcanonical ensemble (NVE) over 16 realizations per state point. To check that finite-size effects are irrelevant, we compare simulations of two system sizes: small systems (S) with $L_x = L_y \approx 13\sigma$, $L_z \approx 31\sigma$ and at least $N = 5000$ particles; and large systems (L) with $L_z \approx 40\sigma$ and at least $N = 7000$ particles (where σ is a typical atomic size, $\sigma \approx 2.7 \text{ \AA}$ for CuZr; precise information is given as Supplemental Information [32]). Our simulations are in equilibrium in the sense that all particles are at the same temperature, and no external field is required to maintain the state, once prepared, in the microcanonical ensemble.

The spatially resolved dynamics can be assessed through the overlap correlation function suggested by the PTS method [11]: the simulation box is discretized into small cubic units of size δ (about $0.52\sigma \approx 1.4 \text{ \AA}$ for CuZr and 0.6σ for the LJBM), and the overlap of configurations a time t apart is calculated as: $q_c(z, t) = \langle \sum_i n_i(t) n_i(0) \delta(z_i - z) \rangle / \langle \sum_i n_i(0) \delta(z_i - z) \rangle$, where $n_i = 1$ if box i at distance z_i from the surface is occupied by an atom and $n_i = 0$ otherwise, and $\langle \cdot \rangle$ denotes an average over the simulation ensemble.

The functions $q_c(z, t)$ follow a standard two-step relaxation pattern of dynamical correlation functions near the glass transition [Fig. 1(c)]: a short-time relaxation to an intermediate-time plateau is followed by stretched-exponential structural relaxation from the plateau. At long times, $q_c(z, t)$ decays to a non-zero z -dependent constant $q_c(z, \infty)$ that represents frozen-in density fluctuations: the introduction of a free surface induces a static density profile $\rho(z)$ [Fig. 1(b)], and we find $q_c(z, \infty) \propto \rho(z)$ [Fig. 1(d)]. This is the expected behavior for a stationary ergodic system, and it marks an important difference of our system to previous PTS analyses where a non-trivial long-time limit of $q_c(z, t)$ signalled a frozen-in nonergodic component of the dynamics. The static overlap evolves smoothly with decreasing temperature, and it decays exponentially towards the bulk density; thus, a *static* correlation length ξ_{stat} can be extracted from fits of the form $q_c(z, \infty) \propto \rho(z) = A(z) \exp(-z/\xi_{\text{stat}}) + \rho(\infty)$, where $\rho(\infty)$ is the density of the bulk liquid. We use the function $A(z) = A_0 \sin(2\pi(z-z_0)/d_p)$ to capture the pronounced surface-induced layering effects seen for CuZr. They are in agreement with experiments on metallic [33] and nonmetallic liquids [34, 35], and grand-canonical MD simulations of liquid films [36]. The LJBM does not show pronounced layering [37], so that there $A(z) = A_0$ is used. In both cases, the static length scale ξ_{stat} increases monotonically and mildly across the temperature range that we investigate (open symbols in Fig. 2). This monotonic increase with decreasing temperature is consistent with the prediction of RFOT and with other computer simulation results [1, 3, 13].

To obtain the *dynamical* correlation length, we parametrize the long-time decay of the overlap correla-

tion function by stretched-exponential functions,

$$q_c(z, t) = q_0(z) \exp[-(t/\tau_{\text{ov}}(z))^{\beta(z)}] + q_c(z, \infty), \quad (1)$$

where $\tau_{\text{ov}}(z)$ is a z -dependent relaxation time. Similar fits have been performed for the collective and self-intermediate scattering function (SISF), and we only discuss the features that are robustly displayed by all relaxation times, taking that of the SISF as a proxy $\tau(z)$; see Fig. 1(d) and Supplemental Material [32].

In the relative enhancement of the mobility $\mu(z) = 1/\tau(z)$, given by $\tau(\infty)/\tau(z) - 1$, there emerge two spatial regimes at low temperature [Fig. 1(e,f)]: close to the surface ($z \lesssim 2\sigma$), an initial exponential decay is identified, whose typical length scale depends only weakly on temperature. This regime corresponds to distances where the static density profile has not yet saturated to its bulk value. An intermediate z -range with a much slower decay opens at lower temperatures ($T \lesssim 1000 \text{ K}$ for CuZr, $T \lesssim 0.45$ for LJ). This intermediate regime expands as T is lowered. Here, $\rho(z) \approx \rho(\infty)$, and thus this is the regime where an intrinsic dynamical correlation length ξ_{dyn} can be extracted from the exponential decay of $\mu(z)$, viz.

$$\mu(z) = C \exp[-z/\xi_{\text{dyn}}] + \mu(\infty). \quad (2)$$

One already anticipates from Fig. 1(e-f) that this dynamical correlation length shows a non-monotonic temperature dependence: curves for intermediate temperature (around $T = 810 \text{ K}$ in the CuZr liquid, and around $T = 0.4$ in the LJ binary mixture) extend further into the bulk than those both at higher and at lower temperatures.

The resulting dynamical correlation lengths ξ_{dyn} display clear maxima at a temperature T_* (Fig. 2). Both above and below T_* , the dynamic and static (symbols with dashed lines in Fig. 2) correlation lengths become similar. In particular, below T_* , ξ_{dyn} decreases towards the smaller static one, ξ_{stat} , again. This is not a finite-size effect: only around the maximum in ξ_{dyn} , some slight effects of system size (in line with those expected from conventional four-point correlations in supercooled liquids [38–40]) are seen that disappear both at higher and at lower temperatures, and thus give additional evidence that the dynamical correlation length peaks at T_* . In both the CuZr and the LJBM system, we note that the peak observed in ξ_{dyn} over ξ_{stat} is at least a factor of 2. It is hence a robust phenomenon across systems with different microscopic interactions and surface features.

We now demonstrate the intimate link of the maximum in the dynamic correlation length *near the surface* with a cross-over point that governs the *bulk* dynamics. Such a link is remarkable, because the point of maximal correlation length, T_* , is clearly above the T_c of MCT, to which candidates of structural changes impacting the relevant dynamical regime have so far been linked. One example is a change in morphology of the CRR as suggested by RFOT [41].

We identify CRR as nearest-neighbor clusters of fast particles in simulations of the *bulk* systems. Following

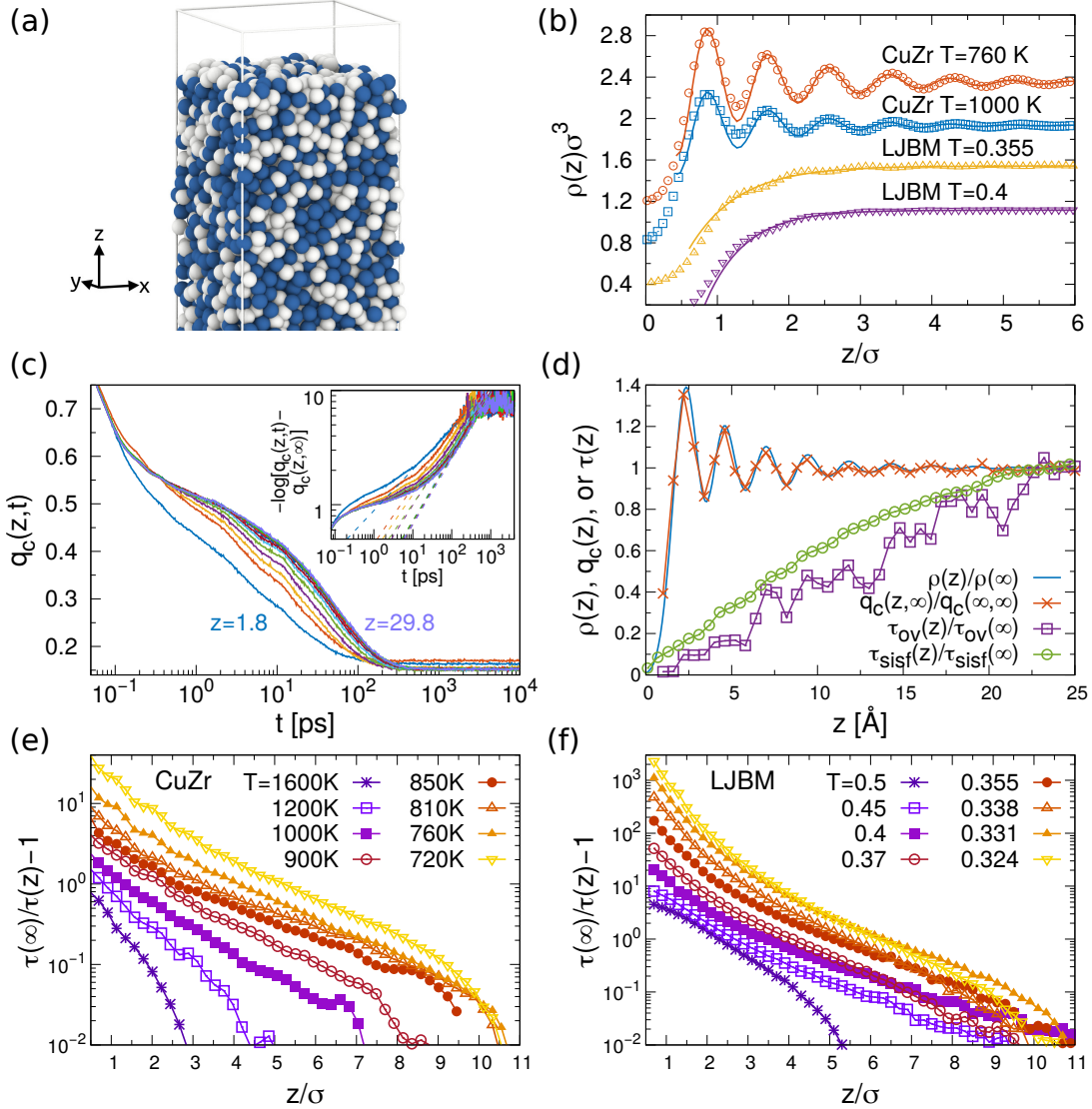


FIG. 1. Characterization of dynamic properties near the surface. (a) Illustrative snapshot of the simulation setup (CuZr system, colors indicating atomic species). (b) Static density profiles $\rho(z)$ as a function of distance z from the surface along the normal into the bulk, for the CuZr liquid and the Lennard-Jones binary mixture (LJBM) (in units of the average atomic radius σ , shifted vertically in steps of $0.4/\sigma^3$ for clarity). Solid lines are fits to extract the static correlation length. (c) Representative decay of the overlap correlation function $q_c(z, t)$ with the distance z to the surface (CuZr; $T = 810$ K). Dashed lines in the inset illustrate stretched-exponential fits of the structural decay, Eq. (1). (d) Static and dynamic parameters characterizing the overlap correlation function (CuZr; $T = 850$ K). The normalized static overlap $q_c(z, \infty)/q_c(\infty, \infty)$ (crosses) follows the normalized density profile $\rho(z)/\rho(\infty)$ (line). The normalized change in the relaxation time $\tau_{ov}(z)/\tau_{ov}(\infty)$ (squares) is shown in comparison to the corresponding quantity obtained from the z -resolved SISF (circles). (e) and (f): Position-dependent relative mobility enhancement $\tau(\infty)/\tau(z) - 1$ (from the layer-resolved SISF) for CuZr and the LJBM.

[42, 43], fast particles are defined as those that during the time interval corresponding to the average structural relaxation time, have moved significantly farther than what is expected from the average mean-squared displacement. Clusters are defined by fast particles closer than the first minimum position in the pair distribution function. To quantify the shape and in particular the anisotropy of these clusters, we consider the ratio of their correlation length to the expected spherical size: In analogy to percolation theory [44], the average cluster correlation length

is given by

$$\xi_{cl}^2 = \sum_s R_{g,s}^2 s^2 P(s) / \sum_s s^2 P(s), \quad (3)$$

where the sums run over the individual clusters of size s , $P(s)$ is the probability of finding a cluster of size s , and $R_{g,s}$ is the radius of gyration of the cluster of size s , defined by $R_{g,s}^2 = \frac{1}{2s^2} \left\langle \sum_{ij \in s} (\vec{r}_i - \vec{r}_j)^2 \right\rangle_s$, where the sum runs over all particles i, j that are part of the cluster, and

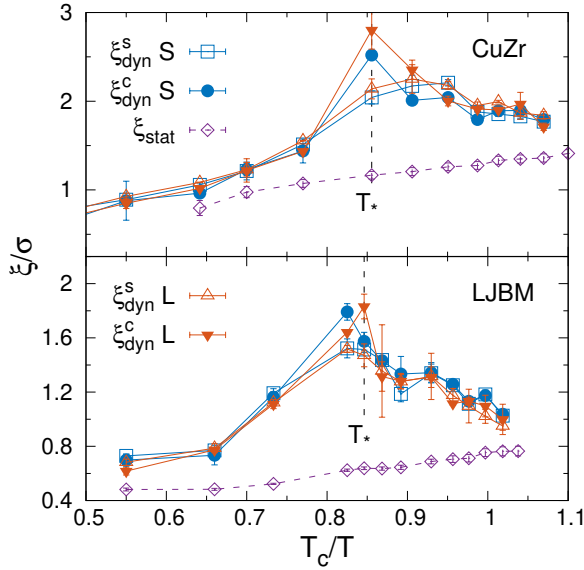


FIG. 2. Temperature dependent static $\xi_{\text{stat}}(T)$ and dynamic correlation lengths $\xi_{\text{dyn}}(T)$ near a free surface for the CuZr (top panel) and the LJBM liquids (bottom panel). The static correlation length ξ_{stat} is extracted from the exponential decay of $\rho(z)$. Values from the self- ($\xi_{\text{dyn}}^{\text{S}}$) and collective- ($\xi_{\text{dyn}}^{\text{C}}$) intermediate scattering functions are shown in systems of two different sizes (S: small systems; L: large systems). The evolution is non-monotonic around a peak temperature T_* indicated by the dashed vertical lines.

$\langle \dots \rangle_s$ denotes the average over all clusters of size s . The expected linear dimension of a spherical cluster of size R_s in turn is defined by $\langle s \rangle = (4\pi/3)\rho_n R_s^3$, where ρ_n is the number density, and $\langle s \rangle = \sum_{s \geq 2} s^2 P(s) / \sum_{s \geq 2} s P(s)$ is the average cluster size. The ratio, ξ_{cl}/R_s , can then be used as a simple proxy to measure the anisotropy of the fast-particle regions.

The aspect ratio of clusters, ξ_{cl}/R_s , exhibits a striking non-monotonic behaviour with temperature change [Fig. 3(a)], with a maximum at the same temperature $T_* > T_c$ where also the dynamical correlations near a free surface show a maximum. Thus we argue that ξ_{dyn} is intimately related to the shape transition of CRR in the bulk.

Typical shapes found for the fast-particle clusters in the bulk are also shown to demonstrate the shape transition [Fig. 3(b–d)]: at high temperatures, clusters are small and of a random-walk like fractal structure. As the temperature is lowered, the clusters increase in size, and at temperatures below T_* , they are relatively compact objects. Around $T = T_*$, the anisotropy is largest: as the clusters grow in average size upon lowering the temperature, this growth first occurs through a string-like extension of the clusters; only below T_* , a more isotropic growth of the clusters is seen. While the string-like motion of atoms is well known in supercooled liquids [42, 43, 45, 46], this is the first report for the shape of CRR transiting back to the compact geometry at low

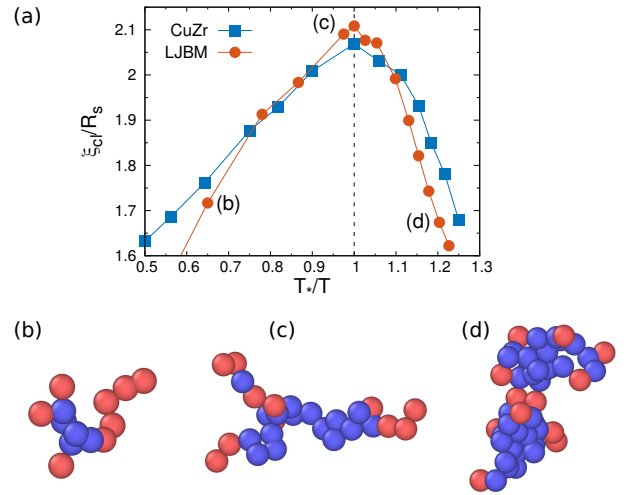


FIG. 3. Characterization of the CRR shape in the bulk liquids. (a), Aspect ratio of fast-particle clusters in the bulk simulations, ξ_{cl}/R_s . The positions of the labels, (b), (c), and (d), correspond to the temperature points at which fast-particle clusters are exemplified in panel (b), (c), and (d), respectively. Particles in blue correspond to the core of the cluster, defined as having more than two fast nearest neighbours, whereas particles shown in red are those having only one or two fast particles as their nearest neighbors.

temperatures in atomic glass formers.

The emergence of large CRR signals heterogeneities in the dynamics that *inter alia* lead to a breakdown of the Stokes–Einstein (SE) relation [39, 47–49]: the fast-particle dominated diffusivity decouples from the bulk relaxation that is governed by the slow particles [50, 51]. While far above T_c a SE relation for the diffusion coefficient of a tracer particle, $D/T \sim \eta^{-1}$ holds well, far below T_c a fractional SE relation emerges, $D/T \sim \eta^{-x}$ with some exponent $x < 1$ (Fig. 4). The maximum anisotropy of CRR at T_* suggests that there, the coupling of fast-particle motion to the bulk dynamics changes, and that this can be connected to the breakdown of the SE relation [3].

Crucially, this allows to provide a clear first-principles definition of T_* . We do so by recalling a recent extension of the asymptotic laws of MCT, the stochastic β -relaxation theory (SBR) [52–54]. It rationalizes the crossover from regular to fractional SE relations as arising from long-wavelength fluctuations in the local dynamical order parameter [55]: above T_c the average dynamics is mean-field liquid-like, and the SE relation results from the realization $\langle 1/\mu \rangle \sim 1/\langle \mu \rangle$. Below T_c , the relaxation dynamics is dominated by rare fluctuations of liquid regions inside a glass-like matrix, and the tail of the order-parameter distribution gives rise to a fractional SE relation, since $\langle 1/\mu \rangle \not\sim 1/\langle \mu \rangle$. SBR describes our data well (solid line in Fig. 4).

Within SBR, we can rigorously identify the point of maximal dynamical correlation, T_* , as the point where the decoupling of fast-particle dominated motion (diffu-

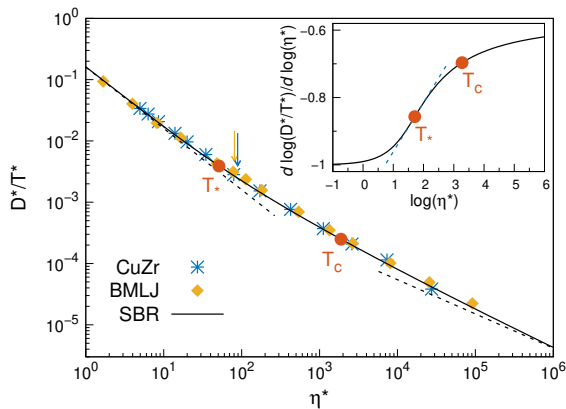


FIG. 4. Stokes–Einstein plot of diffusivity D versus viscosity η (in LJBM units) for the *bulk* liquids, compared with the theoretical prediction from stochastic β -relaxation theory (SBR) (solid line, using the MCT exponent parameter $\lambda = 0.75$). To make data collapse in different systems, D/T and η are scaled to D^*/T^* and η^* in CuZr. Dotted lines are the SBR asymptotes for high and low temperatures, i.e., a regular Stokes–Einstein law, $D^*/T^* \sim \eta^{*-1}$, and a fractional law $D^*/T^* \sim \eta^{*-0.558}$. Red circles mark the MCT- T_c , and T_* predicted from SBR; arrows indicate the approximate maximum positions T_* inferred from ξ_{dyn} for the two simulated systems. We determine T_* within SBR from the point of maximum slope in the SE crossover curve $d \log(D^*/T^*)/d \log \eta^*$ as shown in the inset.

sivity) from the bulk relaxation is most sensitive to fluctuations in the local glassiness of the dynamics. As SBR predicts the logarithmic derivative of D/T as a function of η to cross over from -1 in the ordinary SE regime to $-x$ in the glass, we identify the temperature where this crossover is most rapid as T_* (inset of Fig. 4). At this point, the competition of dynamic fluctuation between the liquid-like regions and the glass-like ones is the strongest. This prediction agrees well with the points where the maximum dynamic correlation and the largest

anisotropy of the CRR locate (see the marked T_* point and arrows in Fig. 4).

In conclusion, we propose supercooled states with a free surface as a convenient model to interrogate spatial correlations in fully equilibrated systems. They show a clear separation of the static and the dynamic correlation lengths. While non-monotonic behavior of a dynamical correlation length was first reported in strongly perturbed systems [5–7], we strikingly find the non-monotonicity also emerges in the vapour-liquid interface, a natural system in equilibrium, for the glass formers of pair-wise or many-body interatomic interaction. The dynamical correlation length displays a clear maximum at a temperature T_* that is associated to the cross-over from liquid-like dynamics to the spatially heterogeneous glass-like dynamics.

We demonstrate that the non-monotonic change in dynamical correlation as measured *near the surface* is linked to a non-monotonic evolution of the aspect ratio of fast-particle clusters *in the bulk*, concomitantly signalled by the breakdown of the Stokes-Einstein relation. Thus the point of maximum dynamical correlations T_* can be identified as the point where the balance of liquid- and glass-like fluctuations in the system is most sensitive to a change in control parameter. In particular the stochastic β -relaxation theory allows to identify T_* in this way as a temperature that is strongly relevant for the dynamics in glass formers – both in bulk and for the formation of glassy films – and that is genuinely distinct from the T_c of MCT.

ACKNOWLEDGMENTS

The authors thank Walter Kob and Clemens Bechinger for their valuable comments. We also appreciate the computer resources provided by the High Performance Computing Center (HPC) of Central South University.

-
- [1] L. Berthier and G. Biroli, *Rev. Mod. Phys.* **83**, 587 (2011).
 - [2] M. D. Ediger, *Annu. Rev. Phys. Chem.* **51**, 99 (2000).
 - [3] E. Flenner, H. Staley, and G. Szamel, *Phys. Rev. Lett.* **112**, 097801 (2014).
 - [4] C. Bennemann, C. Donati, J. Baschnagel, and S. C. Glotzer, *Nature* **399**, 246 (1999).
 - [5] W. Kob, S. Roldán-Vargas, and L. Berthier, *Nat. Phys.* **8**, 164 (2012).
 - [6] G. M. Hocky, L. Berthier, W. Kob, and D. R. Reichman, *Phys. Rev. E* **89**, 052311 (2014).
 - [7] K. H. Nagamanasa, S. Gokhale, A. K. Sood, and R. Ganapathy, *Nat. Phys.* **11**, 403 (2015).
 - [8] C. Lozano, J. R. Gomez-Solano, and C. Bechinger, *Nat. Mater.* **18**, 1118 (2019).
 - [9] B. Li, K. Lou, W. Kob, and S. Granick, *Nature (London)* **587**, 225 (2020).
 - [10] T. R. Kirkpatrick and D. Thirumalai, *Phys. Rev. A* **40**, 1045 (1989).
 - [11] A. Cavagna, T. S. Grigera, and P. Verrocchio, *Phys. Rev. Lett.* **98**, 187801 (2007).
 - [12] G. Biroli, J.-P. Bouchaud, A. Cavagna, T. S. Grigera, and P. Verrocchio, *Nat. Phys.* **4**, 771 (2008).
 - [13] P. Scheidler, W. Kob, and K. Binder, *Eur. Phys. J. E* **12**, 5 (2003).
 - [14] S. Franz and A. Montanari, *J. Phys. A: Math. Theor.* **40**, F251 (2007).
 - [15] B. Zhang and X. Cheng, *Phys. Rev. Lett.* **116**, 098302 (2016).
 - [16] C. Balbuena, M. M. Gianetti, and E. R. Soulé, *J. Chem. Phys.* **150**, 234508 (2019).
 - [17] E. Flenner and G. Szamel, *Nat. Phys.* **8**, 696 (2012).
 - [18] V. Vaibhav and J. Horbach, *Phys. Rev. E* **101**, 022605 (2020).

- [19] D. Jasnow, Rep. Prog. Phys. **47**, 1059 (1984).
- [20] Z. Fakhraai and J. A. Forrest, Science **319**, 600 (2008).
- [21] L. Zhu, C. W. Brian, S. F. Swallen, P. T. Strauss, M. D. Ediger, and L. Yu, Phys. Rev. Lett. **106**, 256103 (2011).
- [22] I. Tanis, K. Karatasos, and T. Salez, J. Phys. Chem. B **123**, 8543 (2019).
- [23] S. F. Swallen, K. L. Kearns, M. K. Mapes, Y. S. Kim, R. J. McMahon, M. D. Ediger, T. Wu, L. Yu, and S. Satija, Science **315**, 353 (2007).
- [24] H.-B. Yu, Y. Luo, and K. Samwer, Adv. Mater. **25**, 5904 (2013).
- [25] S. Singh, M. D. Ediger, and J. J. de Pablo, Nat. Mater. **12**, 139 (2013).
- [26] L. Berthier, P. Charbonneau, E. Flenner, and F. Zamponi, Phys. Rev. Lett. **119**, 188002 (2017).
- [27] P. Luo, C. R. Cao, F. Zhu, Y. M. Lv, Y. H. Liu, P. Wen, H. Y. Bai, G. Vaughan, M. di Michiel, B. Ruta, and W. H. Wang, Nat. Commun. **9**, 1389 (2018).
- [28] L. Chen, C. R. Cao, J. A. Shi, Z. Lu, Y. T. Sun, P. Luo, L. Gu, H. Y. Bai, M. X. Pan, and W. H. Wang, Phys. Rev. Lett. **118**, 016101 (2017).
- [29] W. Kob and H. C. Andersen, Phys. Rev. E **51**, 4626 (1995).
- [30] M. I. Mendeleev, M. J. Kramer, R. T. Ott, D. J. Sordelet, D. Yagodin, and P. Popel, Phil. Mag. **89**, 967 (2009).
- [31] S. Plimpton, J. Comp. Phys. **117**, 1 (1995).
- [32] Supplemental Material.
- [33] O. G. Shpyrko, A. Y. Grigoriev, C. Steimer, P. S. Pershan, B. Lin, M. Meron, T. Graber, J. Gerbhardt, B. Ocko, and M. Deutsch, Phys. Rev. B **70**, 224206 (2004).
- [34] H. Mo, G. Evmenenko, S. Kewalramani, K. Kim, S. N. Ehrlich, and P. Dutta, Phys. Rev. Lett. **96**, 096107 (2006).
- [35] J. Haddad, D. Pontoni, B. M. Murphy, S. Festersen, B. Runge, O. M. Magnussen, H.-G. Steinrueck, H. Reicher, B. M. Ocko, and M. Deutsch, Proc. Natl. Acad. Sci USA **115**, E1100 (2018).
- [36] J. Gao, W. D. Luedtke, and U. Landman, Phys. Rev. Lett. **79**, 705 (1997).
- [37] E. Chacón, M. Reinaldo-Falagán, E. Velasco, and P. Tarazona, Phys. Rev. Lett. **87**, 166101 (2001).
- [38] L. Berthier, G. Biroli, D. Coslovich, W. Kob, and C. Toninelli, Phys. Rev. E **86**, 031502 (2012).
- [39] H. L. Peng and Th. Voigtmann, Phys. Rev. E **94**, 042612 (2016).
- [40] S. Karmakar, C. Dasgupta, and S. Sastry, Phys. Rev. Lett. **105**, 019801 (2010).
- [41] J. D. Stevenson, J. Schmalian, and P. G. Wolynes, Nat. Phys. **2**, 268 (2006).
- [42] Y. Gebremichael, M. Vogel, and S. C. Glotzer, J. Chem. Phys. **120**, 4415 (2004).
- [43] F. W. Starr, J. F. Douglas, and S. Sastry, J. Chem. Phys. **138**, 12A541 (2013).
- [44] T. Nakayama and K. Yakubo, *Fractal Concepts in Condensed Matter Physics* (Springer, 2003).
- [45] C. Donati, J. F. Douglas, W. Kob, S. J. Plimpton, P. H. Poole, and S. C. Glotzer, Phys. Rev. Lett. **80**, 2338 (1998).
- [46] B. A. P. Betancourt, J. F. Douglas, and F. W. Starr, J. Chem. Phys. **140**, 204509 (2014).
- [47] S. Sengupta, S. Karmakar, C. Dasgupta, and S. Sastry, J. Chem. Phys. **138**, 12A548 (2013).
- [48] T. Kawasaki and A. Onuki, Phys. Rev. E **87**, 012312 (2013).
- [49] S. C. Glotzer, V. N. Novikov, and T. B. Schroder, J. Chem. Phys. **112**, 509 (2000).
- [50] S. Sengupta, S. Karmakar, C. Dasgupta, and S. Sastry, J. Chem. Phys. **140**, 224505 (2014).
- [51] H. R. Schober and H. L. Peng, Phys. Rev. E **93**, 052607 (2016).
- [52] T. Rizzo, Phys. Rev. E **87**, 022135 (2013).
- [53] T. Rizzo, EPL **106**, 56003 (2014).
- [54] T. Rizzo, Phys. Rev. B **94**, 014202 (2016).
- [55] T. Rizzo and T. Voigtmann, EPL **111**, 56008 (2015).